

## Massive Galaxy Clusters Like El Gordo Hint at Primordial Quantum Diffusion

Jose María Ezquiaga,<sup>1,2,\*</sup> Juan García-Bellido<sup>3,†</sup> and Vincent Vennin<sup>4,5,‡</sup>

<sup>1</sup>Niels Bohr International Academy, Niels Bohr Institute, Blegdamsvej 17, DK-2100 Copenhagen, Denmark

<sup>2</sup>Kavli Institute for Cosmological Physics and Enrico Fermi Institute, The University of Chicago, Chicago, Illinois 60637, USA

<sup>3</sup>Instituto de Física Teórica UAM-CSIC, Universidad Autónoma de Madrid, Cantoblanco, Madrid, 28049 Spain

<sup>4</sup>Laboratoire de Physique de l'École Normale Supérieure, ENS, Université PSL, CNRS, Sorbonne Université, Université Paris Cité, F-75005 Paris, France

<sup>5</sup>Laboratoire Astroparticule et Cosmologie, CNRS Université de Paris, 10 rue Alice Domon et Léonie Duquet, 75013 Paris, France



(Received 23 July 2022; revised 1 December 2022; accepted 7 February 2023; published 24 March 2023)

It is generally assumed within the standard cosmological model that initial density perturbations are Gaussian at all scales. However, primordial quantum diffusion unavoidably generates non-Gaussian, exponential tails in the distribution of inflationary perturbations. These exponential tails have direct consequences for the formation of collapsed structures in the Universe, as has been studied in the context of primordial black holes. We show that these tails also affect the very-large-scale structures, making heavy clusters like “El Gordo,” or large voids like the one associated with the cosmic microwave background cold spot, more probable. We compute the halo mass function and cluster abundance as a function of redshift in the presence of exponential tails. We find that quantum diffusion generically enlarges the number of heavy clusters and depletes subhalos, an effect that cannot be captured by the famed  $f_{\text{NL}}$  corrections. These late-Universe signatures could, thus, be fingerprints of quantum dynamics during inflation that should be incorporated in  $N$ -body simulations and checked against astrophysical data.

DOI: 10.1103/PhysRevLett.130.121003

*Introduction.*—The standard cosmological model ( $\Lambda$ CDM) provides an excellent fit to high-precision astrophysical and cosmological observations, in particular, the cosmic microwave background (CMB), the large-scale structure (LSS) of the Universe, and the relative abundance of light elements. Its three main ingredients are (i) general relativity and the cosmological principle, (ii) a Universe made of baryonic matter, dark matter, radiation, and dark energy, and (iii) quasi-scale-invariant, Gaussian initial density fluctuations.

However, hints for a few cracks start to emerge at different stages, in the form of moderate statistical tensions in parameter inference, e.g., the local expansion rate [1,2], or via the existence of “extreme” objects or outliers, which are more frequently observed than what  $\Lambda$ CDM predicts. Those may be associated with either an extremely low value of the density field (such as the Eridanus supervoid [3,4], which seems to have a direct connection with the CMB cold spot [5]) or extremely large values of the density field (such as massive galaxy clusters like *El Gordo* [6]—see, however, Ref. [7] for a recent smaller estimate of its mass—and the presence of galaxies and quasistellar objects at extremely high redshifts, where according to standard  $\Lambda$ CDM there should not be any [8,9]). In addition to the early structure formation issues, there are late time mismatches at small scales such as the

substructure problems [10] and the too-big-to-fail and the core-cusp problems [11], which could be alleviated by incorporating baryonic physics [12].

While most attempts to reconcile those potential issues focus on relaxing either the first or the second assumption mentioned above (i.e., modifying the laws of gravity or invoking the existence of additional components in the Universe), a natural strategy to accommodate the existence of extreme objects within the  $\Lambda$ CDM paradigm would be to question the third assumption, namely, the Gaussianity of the primordial density fluctuations. The reason is twofold: Experimentally, there are more extreme objects than what Gaussian tails suggest, pointing toward the existence of heavier tails; theoretically, the typical mechanisms producing primordial cosmological perturbations anyway lead to non-Gaussian tails.

In the early Universe, indeed, vacuum quantum fluctuations are amplified by gravitational instability and stretched to large distances, giving rise to classical fluctuations in the density field, that later collapse into cosmological structures [13]. At leading order in cosmological perturbation theory, it gives rise to Gaussian perturbations, in good agreement with CMB measurements [15]. However, the CMB gives access to large scales only and leaves small scales mostly unconstrained. Moreover, even at large scales, they restrict the statistics of the most likely

fluctuations only; i.e., they reconstruct only the neighborhood of the maximum of the underlying distribution functions and say little about their tails.

Nonetheless, beyond linear order, those tails are expected to be non-Gaussian. The difficulty when characterizing the statistics of those tails is that they require nonperturbative techniques. Perturbative approaches, such as calculations of the bi- or trispectrum, and  $f_{\text{NL}}$ -like parametrizations, are tailored to describe small deviations from Gaussianity around the maximum, not accounting for the tails.

*Quantum diffusion and non-Gaussian tails.*—Recently, nonperturbative techniques have been developed to study how quantum diffusion, the presence of which is inevitable in scenarios where cosmological perturbations have a quantum origin, modifies the expansion dynamics of the Universe and, thus, affects the statistics of density fluctuations. This can be done by combining three approaches to describe the dynamics of super-Hubble degrees of freedom. First is the separate-universe picture [16–19] (which is valid beyond slow roll [20,21]), according to which spatial gradients can be neglected on super-Hubble scales, and each spatial point evolves independently along the dynamics of an unperturbed universe. Second is stochastic inflation [22,23], in which quantum fluctuations act as a stochastic noise on the classical, background evolution of each of these separate universes. Third is the  $\delta N$  formalism [19,24–26], which states that, in each of these separate universes, the local fluctuation in the amount of expansion realized between an initial flat hypersurface and a final hypersurface of uniform energy density is nothing but the curvature perturbation. This gives rise to the stochastic- $\delta N$  formalism [27–32], which provides a nonperturbative scheme to compute the statistics of curvature perturbations on super-Hubble scales. These methods now extend to the calculation of the density contrast and the compaction function [33].

While these techniques recover quasi-Gaussian distributions close to their maximum, with  $f_{\text{NL}}$ -type corrections, they also reveal the existence of systematic exponential tails [33–40], which strongly deviate from the Gaussian profile (such heavy tails were also found in Refs. [41–44] using different methods). More precisely, the distribution function of the first-passage time  $\mathcal{N}$  can be expanded as  $P(\mathcal{N}) = \sum_{n \geq 0} a_n(\Phi) e^{-\Lambda_n \mathcal{N}}$ , in which  $\Lambda_n$  are the eigenvalues of the adjoint Fokker-Planck operator associated with the stochastic problem under consideration and  $a_n(\Phi)$  are coefficients that depend on the initial configuration in field space (here denoted as  $\Phi$ ). Far on the tail, the smallest eigenvalue dominates,  $P(\mathcal{N}) \propto e^{-\Lambda_0 \mathcal{N}}$ , which implies that large perturbations are much more likely than what a Gaussian behavior,  $P_G \propto e^{-\Lambda_0 \mathcal{N}^2}$ , would suggest. In practice, these exponential tails are more important in models where quantum diffusion dominates at some stages of the inflationary dynamics (leading to smaller values of  $\Lambda_0$  and,

hence, heavier tails). Depending on the time at which this happens, they affect structures at different scales. If the fluctuations are large enough, they may even collapse into black holes upon horizon reentry after inflation. This is why non-Gaussian tails have been mostly studied in the context of primordial-black-hole production (see, e.g., Refs. [33,34,37,39,45–50]).

Nonetheless, as we argue here, these heavy tails may also play a key role in the formation of the LSS and point toward potential solutions to some of the problems of  $\Lambda$ CDM. Importantly, while the parameters  $a_n$  and  $\Lambda_n$  depend on the details of the model under consideration, the existence of these exponential tails is ubiquitous and arises in any model where quantum diffusion is at play. In this sense, they are already embedded in the  $\Lambda$ CDM scenario. Therefore, our approach does not rely on extending  $\Lambda$ CDM to solve the above-mentioned issues: Our goal is rather to point out that  $\Lambda$ CDM may already contain the ingredients needed to explain those “anomalous” observations, provided we carefully compute the primordial statistics beyond the perturbative level.

Heavy tails in the form of log-normal distributions are already known to develop on sub-Hubble scales after inflation, due to gravitational collapse [51–53]. However, the effect we are considering here is different: It leads to *primordial* heavy tails, which are present even before Hubble reentry.

*Exponential tails in the primordial statistics of perturbations.*—The details of the stochastic distribution associated with primordial perturbations depend on the specifics of the inflationary model (the number of fields, their potential, their kinetic coupling, etc.). In order to describe the amplitude of fluctuations coarse-grained at a certain scale, one has to convolve the first-passage time distributions against backward distributions of the field value [33,38]. Moreover, one must account for the non-linear mapping between the curvature perturbation and the density contrast [54], which further modifies distribution functions and can also introduce heavy tails [55,56]. In this Letter, we do not aim at deriving predictions for specific models but rather wish to explore generic consequences arising from the presence of heavy tails. This is why, in practice, we consider two normalized templates for the distribution function of the density contrast in comoving threading  $\delta$ :

$$\begin{aligned}
 P_2(\delta_k) &= -\frac{\pi}{2\mu^2} \vartheta_2' \left( \frac{\pi\alpha_k}{2}, e^{-\frac{\pi^2}{\mu^2} \mathcal{D}_k} \right), \\
 P_4(\delta_k) &= \frac{\pi}{2\mu^2 \alpha_k} \vartheta_4' \left( \frac{\pi\alpha_k}{2}, e^{-\frac{\pi^2}{\mu^2} \mathcal{D}_k} \right). \quad (1)
 \end{aligned}$$

In these expressions,  $\delta_k$  denotes the Fourier mode of the density contrast, related to the positive variable  $\mathcal{D}_k$  through the relation  $\delta_k = \mathcal{D}_k - \langle \mathcal{D}_k \rangle$ , where the mean value is taken with respect to the distribution function in question.

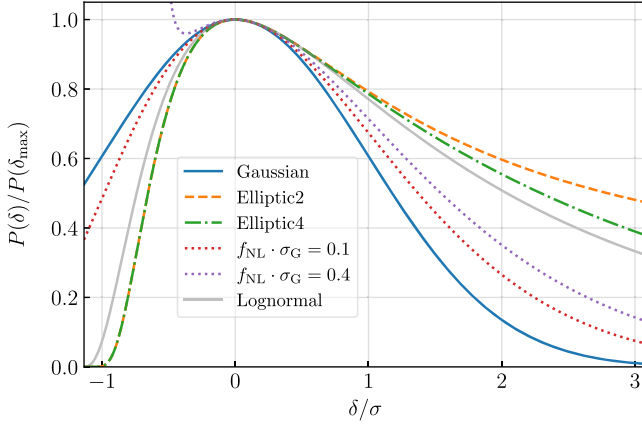


FIG. 1. Gaussian, elliptic, local- $f_{\text{NL}}$ , and log-normal distributions, as a function of  $\delta/\sigma$ , where  $\sigma$  is the standard deviation of the corresponding distribution. The free parameters of those distributions are set such that they all share the same value of  $\sigma$  around the maximum and are given by  $\alpha = 0.5$ ,  $\mu = \pi$ , and  $\sigma = \sqrt{2}\alpha^2$ , with the same  $\alpha$  and  $\mu$  for both elliptic functions. See Supplemental Material [58] for how to match the shape around the maximum.

These distributions depend on two parameters,  $\alpha_k$  and  $\mu$ , the latter being scale independent to reflect the fact that the eigenvalues  $\Lambda_n$  do not depend on the field configuration or, hence, on the scale [35]. Finally,  $\vartheta'_2$  and  $\vartheta'_4$  are the derivatives of the elliptic theta functions of the second and fourth kind, respectively [57]. In what follows, they are referred to as the “elliptic 2” and “elliptic 4” templates, respectively. Such functions are often found in toy models of quantum diffusion [34,35].

The two distributions are displayed in Fig. 1 as a function of  $\delta/\sigma$ , where hereafter  $\sigma$  denotes the standard deviation of the distribution under consideration and where they are compared with a Gaussian distribution, a local  $f_{\text{NL}}$  distribution, and a log-normal distribution. The free parameters of those distributions are set such that they are maximal at the same location and all share the same value of  $\sigma$ ; see Supplemental Material [58], where this procedure is further detailed. Both elliptic profiles are endowed with a heavier upper tail, and with a lighter lower tail, than the Gaussian fit.

The local  $f_{\text{NL}}$  parametrization is defined as

$$\delta(x) = \delta_G(x) + \frac{3}{5} f_{\text{NL}} [\delta_G^2(x) - \sigma_G^2], \quad (2)$$

where  $\delta_G$  has a Gaussian distribution function centered at zero and with dispersion  $\sigma_G \equiv \langle \delta_G^2 \rangle^{1/2}$ . From this expression, one can show that

$$P_{\text{NL}}(\delta) = \frac{1}{\sqrt{2\pi\sigma_G^2\Delta}} \left[ e^{-\frac{25(\sqrt{\Delta}-1)^2}{72f_{\text{NL}}^2\sigma_G^2}} + e^{-\frac{25(\sqrt{\Delta}+1)^2}{72f_{\text{NL}}^2\sigma_G^2}} \right], \quad (3)$$

where  $\Delta(\delta) = 1 + 12/5 f_{\text{NL}} \delta + 36/25 f_{\text{NL}}^2 \sigma_G^2$ . As shown in Fig. 1, although  $f_{\text{NL}}$  correctly describes the non-Gaussian

corrections around the maximum, it fails to capture the highly non-Gaussian tails. Similarly, since  $P_{\text{NL}}$  diverges when  $\delta$  approaches  $-3f_{\text{NL}}\sigma^2/5 - 5/(12f_{\text{NL}})$ , it cannot properly describe the small- $\delta$  statistics [59]. Interestingly, the elliptic functions are more similar to a log-normal distribution than the perturbative  $f_{\text{NL}}$  approximation.

*Implications for the large-scale structure.*—The simplest statistics to be extracted from the primordial density fluctuations is the one-point function, i.e., the number of collapsed objects. Following the Press-Schechter formalism [60], this is given by the probability that  $\delta$  is above a given threshold  $\delta_c$ :  $\beta = P(\delta > \delta_c) = 2 \int_{\delta_c}^{\infty} P(\delta) d\delta$ .  $\delta_c$  depends on the time of reentry of the fluctuations and has been extensively explored in the literature [61–64]. For our purposes it will be enough to fix it to  $\delta_c = 1.6\delta$ , as predicted by linear theory of spherical collapse [65]. From Fig. 1, it is clear that, as  $\nu \equiv \delta_c/\sigma$  increases, the number of collapsed objects is larger in heavy-tailed models than in the Gaussian case.

More precisely, let us study how structures distribute across different masses. This can be achieved with the halo mass function (HMF), defined from the mass fraction  $\beta$  as

$$\frac{dn}{d \ln M} = \frac{\rho_m}{M} \frac{d\beta}{d \ln M} = \frac{\rho_m}{M} \frac{d \ln \sigma^{-1}}{d \ln M} \nu \beta'(\nu), \quad (4)$$

where  $M$  is the mass of the halo,  $\rho_m$  is the energy density of matter, and a prime denotes derivation with respect to  $\nu$ . Previous works have proposed to test  $f_{\text{NL}}$  with the HMF; see, e.g., [66–70]. Here, we extend those results by exploring initial density perturbations with non-Gaussian tails.

Since present observations show a good agreement with the Gaussian hypothesis at galactic scales, we tune the free parameters of all considered distributions such that they peak at the same value and share the same standard deviation (see Supplemental Material [58] for further details). As a consequence, the only difference in Eq. (4) comes from the term  $\beta'(\nu)$ . In a Gaussian distribution, one has  $\beta'_G(\nu) = -2e^{-\nu^2/2}/\sqrt{\pi}$ , and similar expressions can be obtained for the other distributions.

Let us now study the redshift evolution of the number of halos. We can describe the HMF (4) as a function of redshift by writing  $\rho_m(a) = \Omega_m(a)\rho_c$  with  $\Omega_m(a) = \Omega_m/a^3$  and  $\sigma(a) = \sigma(1)D(a)$ , with the growth function  $D(a) = \delta(a)/\delta(1)$  given by [71]  $D(a) \propto a \times {}_2F_1[(w-1)/2w, -1/3w, (6w-5)/6w, 1-1/\Omega_m(a)]$ , where  $w$  is the equation of state of dark energy (set to  $w = -1$ ) and  $a$  is the scale factor. By comparing the HMF at different redshifts with the abundance of massive clusters, we can estimate whether, e.g., El Gordo is a typical cluster or not, at a given redshift.

Our main results are presented in Fig. 2, where we display the HMF for the four distributions under consideration at three redshifts,  $z = 0, 1, 7$ . The bottom panels

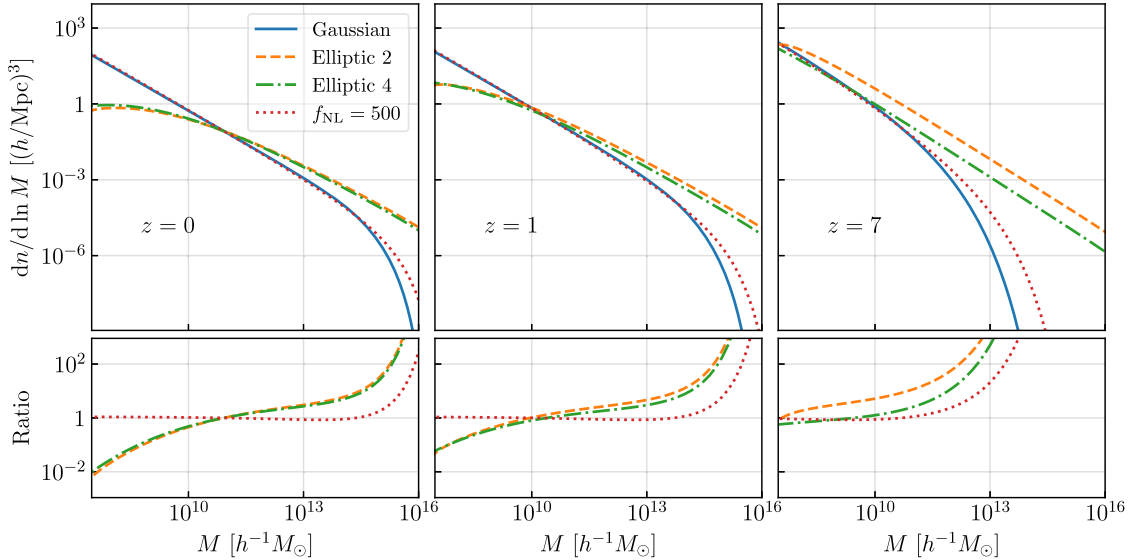


FIG. 2. Halo mass function (i.e., differential number of halos per comoving volume) obtained from different distributions for the primordial density perturbations: Gaussian, elliptic 2 and 4, and local  $f_{\text{NL}}$  (where  $f_{\text{NL}}$  is fixed at the last scattering surface). Each column corresponds to the HMF at a different redshift. The bottom panels show the ratio between the HMF and the Gaussian result. Quantum diffusion affects both low- and high-mass ends of the HMF and become more significant at higher redshifts, making their signatures distinguishable from perturbative non-Gaussianities ( $f_{\text{NL}}$ ). The normalization is fixed to match the Gaussian at  $M = 10^{11} h^{-1} M_{\odot}$  and  $z = 0$ , where  $h$  is the dimensionless Hubble constant,  $h = H_0/(100 \text{ km/s/Mpc})$ .

display the ratio of the HMF with respect to the Gaussian case, with the normalization fixed to the Gaussian at  $M = 10^{11} h^{-1} M_{\odot}$ . At  $z = 0$  we observe two main effects from the exponential tails: an increase in the number of clusters ( $M > 10^{13} M_{\odot}$ ) and a decrease in the number of substructures ( $M < 10^9 M_{\odot}$ ). Interestingly, the  $f_{\text{NL}}$  reconstruction can partially mimic the increase in clusters but not the decrease in substructures. This makes the predictions of quantum diffusion falsifiable. Equally important, the predictions of the elliptic HMF can potentially alleviate the shortcomings of  $\Lambda$ CDM. Moreover, we also observe that the redshift evolution of the HMF is a key discriminator of the nature of the primordial perturbations. An elliptic HMF predicts that more massive objects formed earlier, in agreement with the recent detection of massive, high-redshift objects (see, e.g., [72] for a recent census of the age of young quasars).

In addition to the number of halos per unit mass, it is interesting to compute the number of clusters as a function of redshift. This can be probed directly, for example, with CMB data using the Sunyaev-Zeldovich (SZ) effect [73–75]. Our results are presented in Fig. 3, focusing on clusters with  $M > 10^{15} M_{\odot}$  (see Supplemental Material [58] for the detailed calculation). One can clearly see that, already beyond  $z \sim 1$ , the number of clusters is much enhanced when initial perturbations have heavy tails. This, again, shows the potential of this method to constrain the very early-Universe physics.

Observationally, in most cases we do not have direct access to the HMF but rather to the amount of luminous

matter. One, thus, needs to take into account the astrophysical systematics connecting these two. Recently, constraints on  $f_{\text{NL}}$  have been derived using UV galaxy luminosity functions that marginalize over those systematics [76]. A natural extension of this work would, thus, be to constrain the heavy tails from quantum diffusion with these data. Moreover, the HMF at subgalactic scales could be probed by analyzing the strong lensing rates and magnifications [77].

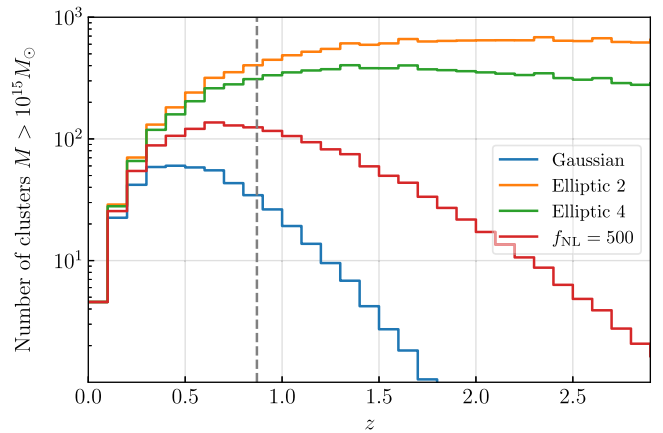


FIG. 3. Number of clusters with mass larger than  $10^{15} M_{\odot}$  in redshift bins of  $\Delta z = 0.1$  as a function of redshift for the Gaussian, elliptic 2 and 4, and  $f_{\text{NL}}$  distributions. The normalization is fixed to the Gaussian case at  $z = 0$ . We highlight with a vertical dashed line the redshift of El Gordo ( $z = 0.87$ ).

*Future prospects.*— $\Lambda$ CDM relies on the assumption of Gaussian initial conditions. Although CMB observations tightly constrain the amount of non-Gaussianities at large scales, little is known about the primordial fluctuations at smaller scales. Several processes in the early Universe could lead to non-Gaussian distributions. Notably, an inevitable exponential tail arises due to quantum diffusion during inflation. In this Letter, we have studied the imprints these heavy tails leave in the number of halos and their mass function. We have found that they enhance the number of heavy clusters and deplete the number of subhalos and that this difference with respect to the standard Gaussian initial conditions becomes more important at high redshift, depending on the strength of quantum diffusion. This could be compared with current SZ catalogs (e.g., Fig. 18 in Ref. [75]) that did not find clusters of  $M > 10^{16} M_{\odot}$  and has a redshift distribution peaking at  $z < 1$ . However, there are outstanding clusters like El Gordo with  $M \sim 3 \times 10^{15} M_{\odot}$  at  $z = 0.87$  [6] and deep voids like the Eridanus supervoid [5], and many more should soon be discovered with the James Webb Space Telescope (JWST) [78], Euclid [79], and the Vera Rubin Observatory [80].

Let us note that the effect of quantum diffusion is similar to having a log-normal initial density distribution. Such log-normal profiles are indeed typically obtained from Gaussian initial conditions due to nonlinear gravitational collapse [51]. In fact, to speed up the computation, many  $N$ -body codes start their evolution with an already log-normal distribution [81,82]. Here, we find that nonlinear growth occurs at much earlier times, as soon as non-Gaussian tails are present. This leaves specific features in the redshift dependence of the statistics: For high-redshift galaxies we expect highly non-Gaussian statistics, much beyond what would be expected from nonlinear gravitational collapse in such a short time.

Using the HMF to probe primordial Universe physics requires further developments on various fronts. From the observational side, we need to understand the systematics behind high-mass supergalactic structures at low and high redshifts, which Euclid [79] and JWST [78] observations may help to alleviate, as well as issues with baryonic physics and halo occupation distributions. The HMF is sensitive to the one-point statistics of the density field only, but it would also be interesting to consider observables probing non-Gaussianities in higher correlators. From the theoretical side, we need to implement realistic physical models in our pipeline and go beyond the simple phenomenological prescription adopted here (although this is not expected to alter our qualitative conclusions, it matters for quantitative details). Finally, on the numerical side, it would be necessary to run  $N$ -body simulations with non-Gaussian initial conditions of the type described above.

Altogether, we have demonstrated the impact of quantum diffusion on the LSS and how the HMF and cluster

abundances can probe early-Universe physics. More importantly, we have shown that, within the standard cosmological model itself, quantum diffusion is inevitable during inflation, and some of the current tensions can be alleviated thanks to the non-Gaussian nature of the tails of primordial perturbations.

J. G. B. acknowledges funding from the Research Project No. PGC2018-094773-B-C32 (MINECO-FEDER) and the Centro de Excelencia Severo Ochoa Program CEX2020-001007-S. J. M. E. is supported by the European Union's Horizon 2020 research and innovation program under the Marie Skłodowska-Curie Grant Agreement No. 847523 INTERACTIONS, and by VILLUM FONDEN (Grant No. 53101 and 37766). He was also supported by NASA through the NASA Hubble Fellowship Grant No. HST-HF2-51435.001-A awarded by the Space Telescope Science Institute, which is operated by the Association of Universities for Research in Astronomy, Inc., for NASA, under Contract No. NAS5-26555; and by the Kavli Institute for Cosmological Physics through an endowment from the Kavli Foundation and its founder Fred Kavli.

\*jose.ezquiaga@nbi.ku.dk

†juan.garciabellido@uam.es

‡vincent.vennin@ens.fr

- [1] W. L. Freedman, *Nat. Astron.* **1**, 0121 (2017).
- [2] L. Verde, T. Treu, and A. G. Riess, *Nat. Astron.* **3**, 891 (2019).
- [3] F. Finelli, J. García-Bellido, A. Kovács, F. Paci, and I. Szapudi, *Mon. Not. R. Astron. Soc.* **455**, 1246 (2016).
- [4] A. Kovács and J. García-Bellido, *Mon. Not. R. Astron. Soc.* **462**, 1882 (2016).
- [5] A. Kovács *et al.*, *Mon. Not. R. Astron. Soc.* **510**, 216 (2022).
- [6] E. Asencio, I. Banik, and P. Kroupa, *Mon. Not. R. Astron. Soc.* **500**, 5249 (2020).
- [7] J. Kim, M. J. Jee, J. P. Hughes, M. Yoon, K. HyeonHan, F. Menanteau, C. Sifton, L. Hovey, and P. Arunachalam, *Astrophys. J.* **923**, 101 (2021).
- [8] A. H. Gonzalez, S. A. Stanford, M. Brodwin, C. Fedeli, A. Dey, P. R. M. Eisenhardt, C. Mancone, D. Stern, and G. Zeimann, *Astrophys. J.* **753**, 163 (2012).
- [9] S. L. Finkelstein *et al.*, *Nature (London)* **502**, 524 (2013).
- [10] A. Del Popolo and M. Le Delliou, *Galaxies* **5**, 17 (2017).
- [11] O. Newton, M. Cautun, A. Jenkins, C. S. Frenk, and J. Helly, *Mon. Not. R. Astron. Soc.* **479**, 2853 (2018).
- [12] J. Zavala and C. S. Frenk, *Galaxies* **7**, 81 (2019).
- [13] This mechanism is mostly studied in the context of inflation, but it also operates in most of its alternatives [14].
- [14] R. H. Brandenberger, *Int. J. Mod. Phys. Conf. Ser.* **01**, 67 (2011).
- [15] Y. Akrami *et al.* (Planck Collaboration), *Astron. Astrophys.* **641**, A9 (2020).
- [16] D. Wands, K. A. Malik, D. H. Lyth, and A. R. Liddle, *Phys. Rev. D* **62**, 043527 (2000).

- [17] I. M. Khalatnikov and A. Y. Kamenshchik, *Classical Quantum Gravity* **19**, 3845 (2002).
- [18] D. H. Lyth and D. Wands, *Phys. Rev. D* **68**, 103515 (2003).
- [19] D. H. Lyth, K. A. Malik, and M. Sasaki, *J. Cosmol. Astropart. Phys.* **05** (2005) 004.
- [20] C. Pattison, V. Vennin, H. Assadullahi, and D. Wands, *J. Cosmol. Astropart. Phys.* **07** (2019) 031.
- [21] D. Artigas, J. Grain, and V. Vennin, *J. Cosmol. Astropart. Phys.* **02** (2022) 001.
- [22] A. A. Starobinsky, *Phys. Lett.* **117B**, 175 (1982).
- [23] A. A. Starobinsky, *Lect. Notes Phys.* **246**, 107 (1986).
- [24] M. Sasaki and E. D. Stewart, *Prog. Theor. Phys.* **95**, 71 (1996).
- [25] M. Sasaki and T. Tanaka, *Prog. Theor. Phys.* **99**, 763 (1998).
- [26] D. H. Lyth and Y. Rodriguez, *Phys. Rev. Lett.* **95**, 121302 (2005).
- [27] K. Enqvist, S. Nurmi, D. Podolsky, and G. I. Rigopoulos, *J. Cosmol. Astropart. Phys.* **04** (2008) 025.
- [28] T. Fujita, M. Kawasaki, Y. Tada, and T. Takesako, *J. Cosmol. Astropart. Phys.* **12** (2013) 036.
- [29] T. Fujita, M. Kawasaki, and Y. Tada, *J. Cosmol. Astropart. Phys.* **10** (2014) 030.
- [30] V. Vennin and A. A. Starobinsky, *Eur. Phys. J. C* **75**, 413 (2015).
- [31] V. Vennin, H. Assadullahi, H. Firouzjahi, M. Noorbala, and D. Wands, *Phys. Rev. Lett.* **118**, 031301 (2017).
- [32] H. Firouzjahi, A. Nassiri-Rad, and M. Noorbala, *J. Cosmol. Astropart. Phys.* **01** (2019) 040.
- [33] Y. Tada and V. Vennin, *J. Cosmol. Astropart. Phys.* **02** (2022) 021.
- [34] C. Pattison, V. Vennin, H. Assadullahi, and D. Wands, *J. Cosmol. Astropart. Phys.* **10** (2017) 046.
- [35] J. M. Ezquiaga, J. García-Bellido, and V. Vennin, *J. Cosmol. Astropart. Phys.* **03** (2020) 029.
- [36] V. Vennin, Habilitation thesis, 2020, arXiv:2009.08715.
- [37] D. G. Figueroa, S. Raatikainen, S. Rasanen, and E. Tomberg, *Phys. Rev. Lett.* **127**, 101302 (2021).
- [38] K. Ando and V. Vennin, *J. Cosmol. Astropart. Phys.* **04** (2021) 057.
- [39] C. Pattison, V. Vennin, D. Wands, and H. Assadullahi, *J. Cosmol. Astropart. Phys.* **04** (2021) 080.
- [40] G. Rigopoulos and A. Wilkins, *J. Cosmol. Astropart. Phys.* **12** (2021) 027.
- [41] G. Panagopoulos and E. Silverstein, arXiv:1906.02827.
- [42] A. Achúcarro, S. Céspedes, A.-C. Davis, and G. A. Palma, *J. High Energy Phys.* **05** (2022) 052.
- [43] F. Kuhnel and D. J. Schwarz, arXiv:2101.10340.
- [44] Y.-F. Cai, X.-H. Ma, M. Sasaki, D.-G. Wang, and Z. Zhou, *J. Cosmol. Astropart. Phys.* **12** (2022) 034.
- [45] S. Clesse and J. García-Bellido, *Phys. Rev. D* **92**, 023524 (2015).
- [46] M. Kawasaki and Y. Tada, *J. Cosmol. Astropart. Phys.* **08** (2016) 041.
- [47] J. M. Ezquiaga and J. García-Bellido, *J. Cosmol. Astropart. Phys.* **08** (2018) 018.
- [48] M. Biagetti, G. Franciolini, A. Kehagias, and A. Riotto, *J. Cosmol. Astropart. Phys.* **07** (2018) 032.
- [49] D. G. Figueroa, S. Raatikainen, S. Rasanen, and E. Tomberg, *J. Cosmol. Astropart. Phys.* **05** (2022) 027.
- [50] N. Kitajima, Y. Tada, S. Yokoyama, and C.-M. Yoo, *J. Cosmol. Astropart. Phys.* **10** (2021) 053.
- [51] P. Coles and B. Jones, *Mon. Not. R. Astron. Soc.* **248**, 1 (1991).
- [52] A. Taruya, M. Takada, T. Hamana, I. Kayo, and T. Futamase, *Astrophys. J.* **571**, 638 (2002).
- [53] S. Hilbert, J. Hartlap, and P. Schneider, *Astron. Astrophys.* **536**, A85 (2011).
- [54] I. Musco, *Phys. Rev. D* **100**, 123524 (2019).
- [55] M. Biagetti, V. De Luca, G. Franciolini, A. Kehagias, and A. Riotto, *Phys. Lett. B* **820**, 136602 (2021).
- [56] V. De Luca and A. Riotto, arXiv:2201.09008.
- [57] F. W. J. Olver, D. W. Lozier, R. F. Boisvert, and C. W. Clark, *The NIST Handbook of Mathematical Functions* (Cambridge University Press, Cambridge, England, 2010), ISBN 9780521140638, 0521140633, 9780521192255, 0521192250.
- [58] See Supplemental Material at <http://link.aps.org/supplemental/10.1103/PhysRevLett.130.121003> for technical details supporting the results presented in the main text.
- [59] The local  $f_{\text{NL}}$  in Eq. (2) is assumed to be constant and, thus, cannot reproduce the scale dependence of the amplitude of the tails that comes from the fact that quantum diffusion has a different effect at different points of the inflationary evolution. Other formulations of primordial non-Gaussianity take into account the “scale dependence” of  $f_{\text{NL}}$  through calculations of the full bispectrum, but they would still be perturbative.
- [60] W. H. Press and P. Schechter, *Astrophys. J.* **187**, 425 (1974).
- [61] T. Harada, C.-M. Yoo, and K. Kohri, *Phys. Rev. D* **88**, 084051 (2013); **89**, 029903(E) (2014).
- [62] S. Young, C. T. Byrnes, and M. Sasaki, *J. Cosmol. Astropart. Phys.* **07** (2014) 045.
- [63] C. Germani and I. Musco, *Phys. Rev. Lett.* **122**, 141302 (2019).
- [64] C.-M. Yoo, T. Harada, J. Garriga, and K. Kohri, *Prog. Theor. Exp. Phys.* **2018**, 123E01 (2018).
- [65] P. J. E. Peebles, *The Large-Scale Structure of the Universe* (Princeton University Press, 1980).
- [66] S. Matarrese, L. Verde, and R. Jimenez, *Astrophys. J.* **541**, 10 (2000).
- [67] N. Dalal, O. Dore, D. Huterer, and A. Shirokov, *Phys. Rev. D* **77**, 123514 (2008).
- [68] M. LoVerde and K. M. Smith, *J. Cosmol. Astropart. Phys.* **08** (2011) 003.
- [69] S. Yokoyama, N. Sugiyama, S. Zaroubi, and J. Silk, *Mon. Not. R. Astron. Soc.* **417**, 1074 (2011).
- [70] A. Moradinezhad Dizgah, M. Biagetti, E. Sefusatti, V. Desjacques, and J. Noreña, *J. Cosmol. Astropart. Phys.* **05** (2021) 015.
- [71] A. Bueno belloso, J. Garcia-Bellido, and D. Sapone, *J. Cosmol. Astropart. Phys.* **10** (2011) 010.
- [72] A.-C. Eilers, J. F. Hennawi, F. B. Davies, and R. A. Simcoe, arXiv:2106.04586.
- [73] P. A. R. Ade *et al.* (Planck Collaboration), *Astron. Astrophys.* **594**, A27 (2016).
- [74] L. E. Bleem *et al.* (SPT and DES Collaborations), *Astrophys. J. Suppl. Ser.* **247**, 25 (2020).
- [75] M. Hilton *et al.* (ACT and DES Collaborations), *Astrophys. J. Suppl. Ser.* **253**, 3 (2021).

- [76] N. Sabti, J. B. Muñoz, and D. Blas, *J. Cosmol. Astropart. Phys.* **01** (2021) 010.
- [77] D. Gilman, A. Benson, J. Bovy, S. Birrer, T. Treu, and A. Nierenberg, *Mon. Not. R. Astron. Soc.* **512**, 3163 (2022).
- [78] J. P. Gardner *et al.*, *Space Sci. Rev.* **123**, 485 (2006).
- [79] L. Amendola *et al.*, *Living Rev. Relativity* **21**, 2 (2018).
- [80] V. Ivezić *et al.* (LSST Collaboration), *Astrophys. J.* **873**, 111 (2019).
- [81] A. Agrawal, R. Makiya, C.-T. Chiang, D. Jeong, S. Saito, and E. Komatsu, *J. Cosmol. Astropart. Phys.* **10** (2017) 003.
- [82] C. Ramírez-Pérez, J. Sanchez, D. Alonso, and A. Font-Ribera, arXiv:2111.05069.